Nanoparticles and Nanosheets of Aromatic Polyimides via Polycondensation in Controlled Pore Geometries

Matthijs Groenewolt, Arne Thomas, and Markus Antonietti*

Max Planck Institute of Colloids and Interfaces, Research Campus Golm, Am Mühlenberg 1, D-14476 Golm, Germany

Received December 1, 2003; Revised Manuscript Received April 1, 2004

ABSTRACT: Nanoparticles and nanosheets of a high-performance aromatic polyimide can be synthesized via a simple monomer adsorption/polycondensation process inside the pores of specially selected mesoporous silica monoliths. The morphology of the pores directly controls the shape of the resulting polymer nanostructures. About perfect replication was found for both silicas under consideration: one a mesoporous silica with spherical pores with a diameter of 13 nm and another with a lamellar pore morphology with ca. 2 nm thickness. The resulting polymer structures were analyzed by TEM, SFM, thermogravimetric analysis, IR spectroscopy, and X-ray scattering, and the generation of a pure nanocrystalline polyimide was verified.

Introduction

Starting from the invention of mesoporous silica in 1992[1] and due to their availability with a wide range of regular pore sizes and connectivities, experiments to use their pore system as a mold to nanostructure a third type of material have become increasingly popular. Early work of Mallouk[2] started with the replication of zeolithic pore structures into phenol−formaldehyde type resins, whereas Göltner and Attard shaped polystyrene/divinylbenzene resins to mesoporous polymers by silica templated by nonionic surfactants.[3,4] Using appropriate carbon precursor polymers, Ryoo and Joo et al. were able to generate nicely ordered mesoporous carbon replicas by a replication/carbonization sequence.[5,6] Another class of experiments highlighting the potential of such replication techniques was the generation of oriented fibers of a conducting polymer, polyaniline, within the oriented hexagonal channels of a MCM41 host,[7] leading to nanowires with high conductance. Tolbert et al.[8,9] were able to extend this principle to photoluminescent conducting polymers, leading to oriented optoelectronic properties.

In the present paper, we want to make use of this "pore replication" (or "nanoreactor") principle for building nanostructures of another interesting class of polymers, the aromatic polyimides. Those polymers are thermally stable until 500 °C and chemically very inert in most conditions and show extraordinary mechanical properties. They are ideal polymer candidates for a number of nanotechnology applications but are hardly processable.[10] This is why colloidal polyimide particles, either spheres (for the sintering toward coatings or as fillers) or nanorods/nanoplates (as fillers and for composite materials), would be highly attractive. Nanopore replication is currently out of range to become an industrial process, but the resulting structures may serve as models to learn about the behavior of those crystalline/liquid crystalline polymers when single dimensions are reduced toward the scale of a few nanometers.

This is why we report on the synthesis of narrowly distributed polyimide nanospheres with 13 nm diameter and of polyimide nanosheets with 2 nm thickness; polyimide formation will be proven by IR spectroscopy, X-ray analysis, and thermogravimetry, whereas the nanostructure is confirmed by transmission electron microscopy (TEM) and atomic force microscopy (AFM).

Experimental Section

The polyimide was synthesized by polycondensation of *p*-phenylenediamine and pyromellithic dianhydride (benzene−1,2,4,5-tetracarboxylic dianhydride) in DMF. In the first polymerization step a polyamide is formed which can be converted into the polyimide by heating to 300 °C in the second step. The polymerization steps are shown in Scheme 1.

Keeping the reaction spatially confined, all polymerization steps were carried out in the pores of mesoporous silica. The synthesis of the silica materials is described elsewhere.[11,12] Both are synthesized via the nanocasting route,[13] using an organic self-organizing template and a liquid silica precursor. For the silica with spherical pores, poly(ethylene-*co*-butylene)-*block*-poly(ethylene oxide) was used as template. After removal of the template through calcination, a mesoporous silica with spherical pores ordered in a face-centered-cubic (fcc) type arrangement is obtained.

For the silica with regular slit pores, the cholesteric phases of hydroxypropylcellulose were used as a template. Here, the cellulose chains form ca. 2 nm thick layers, which are quite stiff and regularly packed.[11] It is important to note that those slit pores, presumably due to rare pillar defects, do not collapse throughout calcination and removal of the template.

In a typical polymer synthesis a 1.0 M solution of the amine is cooled to −60 °C, and the same amount of a 1.0 M solution of the anhydride in DMF and the monolith of the mesoporous silica are added together simultanously. After 10 min it was assumed that the pores are filled with the monomers and the solvent molecules, and the monolith was taken out of the solution and washed two times by dipping it in pure DMF for 30 s to remove surface adsorbed polymer. After tempering the polymer−silica hybrid at 80 °C for 3 h for polyamide precondensation, the monolith was heated to 300 °C to remove the DMF and to form the polyimide. The silica material was removed with hydrofluoric acid solution (48 wt % in water) at room temperature. A more efficient removal of the silica was observed by grinding the hybrid material before the HF treatment. After removing the silica material, glossy yellow powders of polyimide are obtained.

The obtained polyimide was characterized by TEM, AFM, TGA, WAXS, and IR spectroscopy.

Transmission electron microscopy (TEM) images were taken with a Zeiss EM 912Ω at an acceleration voltage of 120 kV. Samples were ground in a ball mill and taken up in acetone.

10.1021/ma035804o CCC: $27.50
Published on Web 05/11/2004

Scheme 1

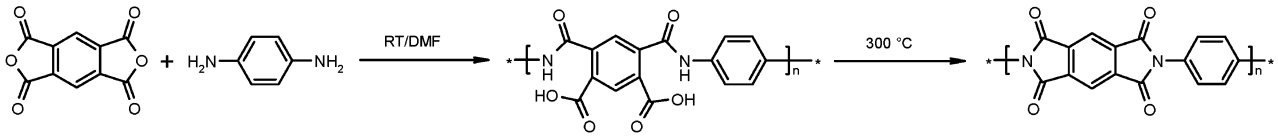

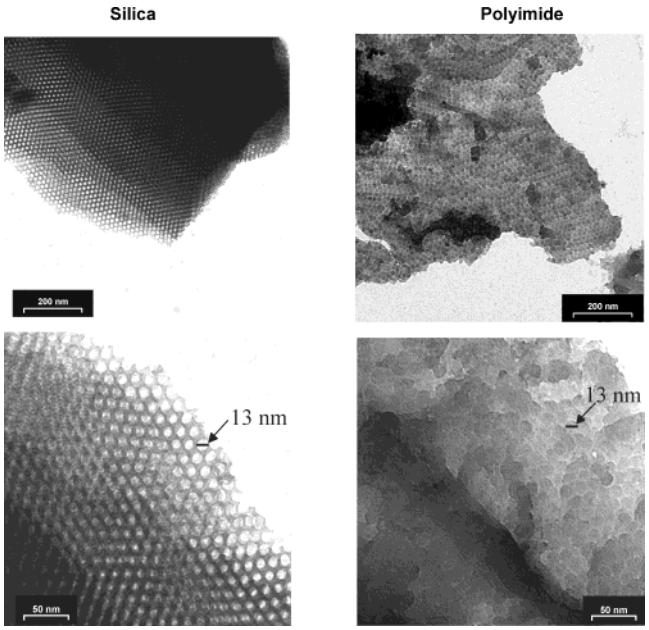

Figure 1. TEM micrographs of the pore structure of the silicas synthesized with block copolymer micelles as template (left) and the resulting polyimide replicas (right).

One droplet of the suspension was applied to a 400 mesh carbon-coated copper grid and left to dry in air.

Tapping mode atomic force microscopy (AFM) images were recorded with a multimode AFM from Vecco Instruments employing Olympus microcantilevers (resonance frequency: 300 kHz; force constant: 42 N/m). The samples were redispersed in water with ultrasonication, and one droplet was spin-coated on a freshly prepared mica substrate.

X-ray data were recorded with a Siemens D8 diffractometer equipped with a Sol X, SI solid-state detector, using Cu Kα radiaton in a symmetric reflection setup.

The IR spectrum was collected with a BIORAD FTS 6000 FTIR spectrometer, equipped with a attenuated total reflection (ATR) setup.

Thermogravimetric analysis has been carried out using a NETZSCH TG209. The heating rate was 20 K/min. The measurements were carried out under an air atmosphere.

Results and Discussion

The described preparation yields in a fine, free-flowing, glossy yellow polymer powder. The nanometric texture of this powder is revealed in TEM experiments. Figure 1 compares the structure of the original template and the structure of the resulting colloidal polyimide replicas. The TEM micrographs clearly indicate that the spherical shape and the diameter of the pores are reflected into polyimide particles of similar size. This provides in general the possibility to tailor the particle diameter and shape by varying the silica matrix only. As shown in the micrographs, the adjacent pore arrangement seems to be reproduced in the packing of the particles. On the basis of these micrographs, it is uncertain whether the particles are separated and only closed-packed (as it could be expected for spherical particles of that small dispersity) or whether the pore interconnections have been replicated, too. As the mesopores of the silica are connected via smaller micropores,[14] which also are involved while filling the pores with the reactants, polymerization in these pores could in principle lead to particles' interconnections. This was for instance found for carbon replicas of SBA15. The diameter of these micropores ($d < 2$ nm) in our case is on the scale of hydrated poly(ethylene glycol) chains; i.e., connections, if they exist, should be constituted of single polyimide chains. The fact that the isolated product is a powder and did not adopt the shape of the monolith indeed proves that those interconnections, if existing, are rare.

To get additional information about the structure of the particles, AFM was used. The AFM pictures indicate regions of isolated particles, beside regions where the particles are close-packed. The dense regions show the standard fcc arrangement of 13 nm sized particles, plus an additional species which sits on top as well as on the steps of the structure. These look like "oily" nanodroplets, being definitely more deformed then the other nanoparticles. We can only speculate about the origin of those species; they might be low molecular weight species trapped in the micropore system which underwent coalescence after removal of the templates or fractured polyimide shells, as delineated below. The "dilute" regions of the AFM pictures show both single spheres as well as smaller aggregates with constant height. A quantitative evaluation of the smaller dots gives a size of 13 ± 0.2 nm, with a height of ca. 1.6 ± 0.3 nm. This is certainly not consistent with a model of massive nanospheres that are fused or connected, as might be inferred from the TEM micrographs in Figure 1. It also must be stated that the morphology of the isolated spheres is in general less defined than the one of the tightly packed counterparts, which indicates a potential problem with sampling, as spheres of different quality are deposited at different places of the film. This is, however, not unusual for polymer colloids. We can, however, excluded impurities and contaminations to be responsible for this effect, as the structures are found in all samples with a rate much higher than we know from the standard impurity artifacts.

A quantitative discussion is somewhat hindered that we have impregnated the monolith with the monomers, which certainly will enrich due to adsorption onto the silica surface, as it was also observed for the anilinium species.[7] As we started with a 1 M solution, the filling of the pores is at least with 14.8 wt % monomer, after condensation revealing at least 14.0 wt % polymer. One explanation for the observed particle size and morphologies could be that the monomers are preferentially located at the pore walls, so that the polymerization occurs mainly on the silica surface. This process would lead to hollow polyimide particles with a minimal molecular weight of 101 500 g/mol, a diameter of 13 nm, and a minimal numerical shell thickness of 0.3 nm; this is the cross section of a single PI chain. As we observe the aromatic stacking peak at $2\Theta = 27°$, it can be assumed that the PI chains sit nematically ordered within the surface (Figure 4).

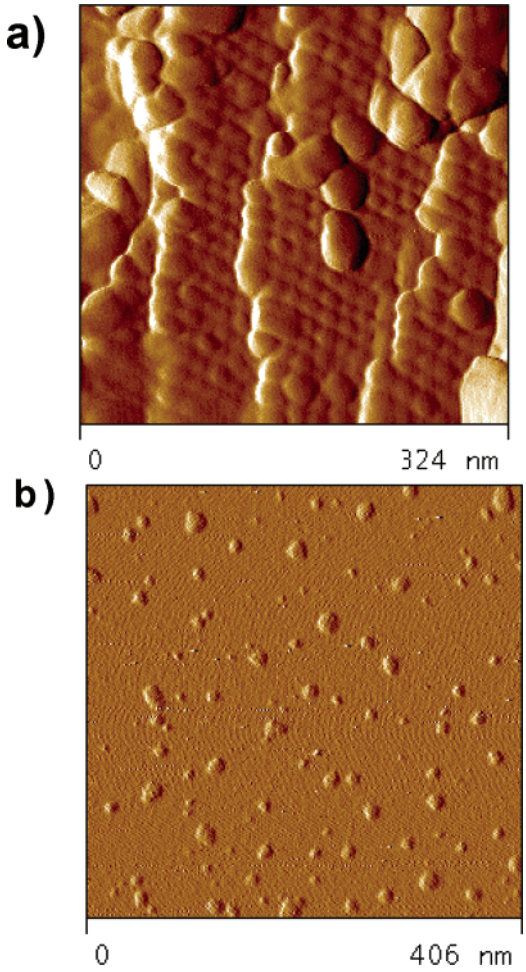

Figure 2. AFM pictures of the spherical polyimide particles: (a) densely packed regions; (b) isolated particles (shown are the amplitude pictures).

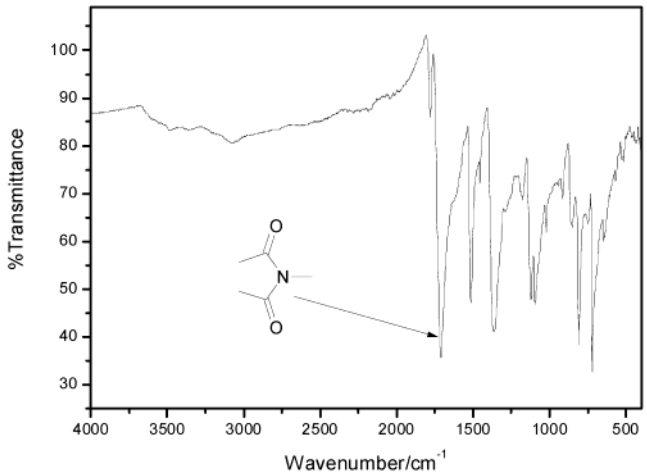

Figure 3. IR spectra of the polyimide particles. Pointed out is the peak of the imide group at 1700 cm^{-1}.

We, however, also cannot exclude the possibility that, at the applied very high temperatures, after removal of the solvent the formed oligomers undergo redistribution and pore condensation in special regions of the silica only. In this case, we would end up with massive spheres and hollow, nonreplicated pores.

The chemical architecture of the polymer can be analyzed by IR spectroscopy of the isolated powder. The IR spectra (Figure 3) show the typical peaks for an aromatic polyimide and confirm the proposed structure. The given aromatic polyimide is expected to be semicrystalline in the bulk. This could be confirmed by WAXS measurements which were carried out to detect the crystallinity in the particles (Figure 4). The WAXS diffractogram also supports the polyimide structure. The found scattering peaks overlap with a reference sample prepared in the bulk. The peaks are slightly broadened, as it is well-known for nanoparticles. The width of the peaks also prevents a more detailed discussion of local arrangements.

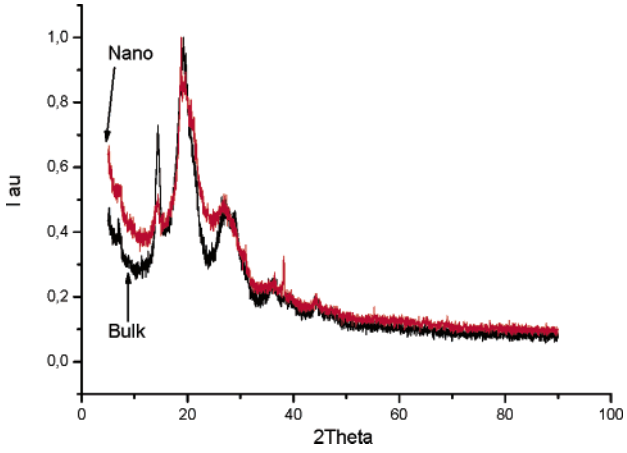

Figure 4. WAXS diffractograms characterizing the crystallinity of the bulk and the nanometer-sized polyimide.

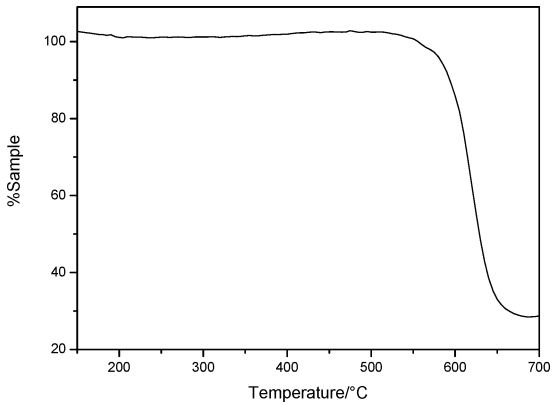

Figure 5. TGA of the polyimide polymerized in a porous silica.

The high-temperature stability of the resulting nanoparticles can be quantified by TGA (Figure 5). The TGA shows that the particles are thermically stable up to 550 °C. The decomposition starts between 560 and 580 °C. This indicates that the high-temperature resistance, one relevant property for the application of this type of polymer, is also maintained in the nanosized particles. In the present sample, TGA also shows a nondegradable fraction of 30 wt % which is essentially carbon from the polyimide plus some adsorbed silica. Because of the risks involved while working with more aggressive versions of HF, we refrained from strictly removing silica.

The most extended structures of the present set of experiments have been produced in the lamellar, sheetlike pores of the hydroxypropylcellulose-templated silica. Figure 6a shows the original silica (where the highly parallel channel structure is hardly visible due to its small size) compared to the structure of the isolated polyimide replicas depicted in Figure 6b,c.

Polyimide sheets with an average thickness of 2.0 nm become visible in the side view. This is in good agree-

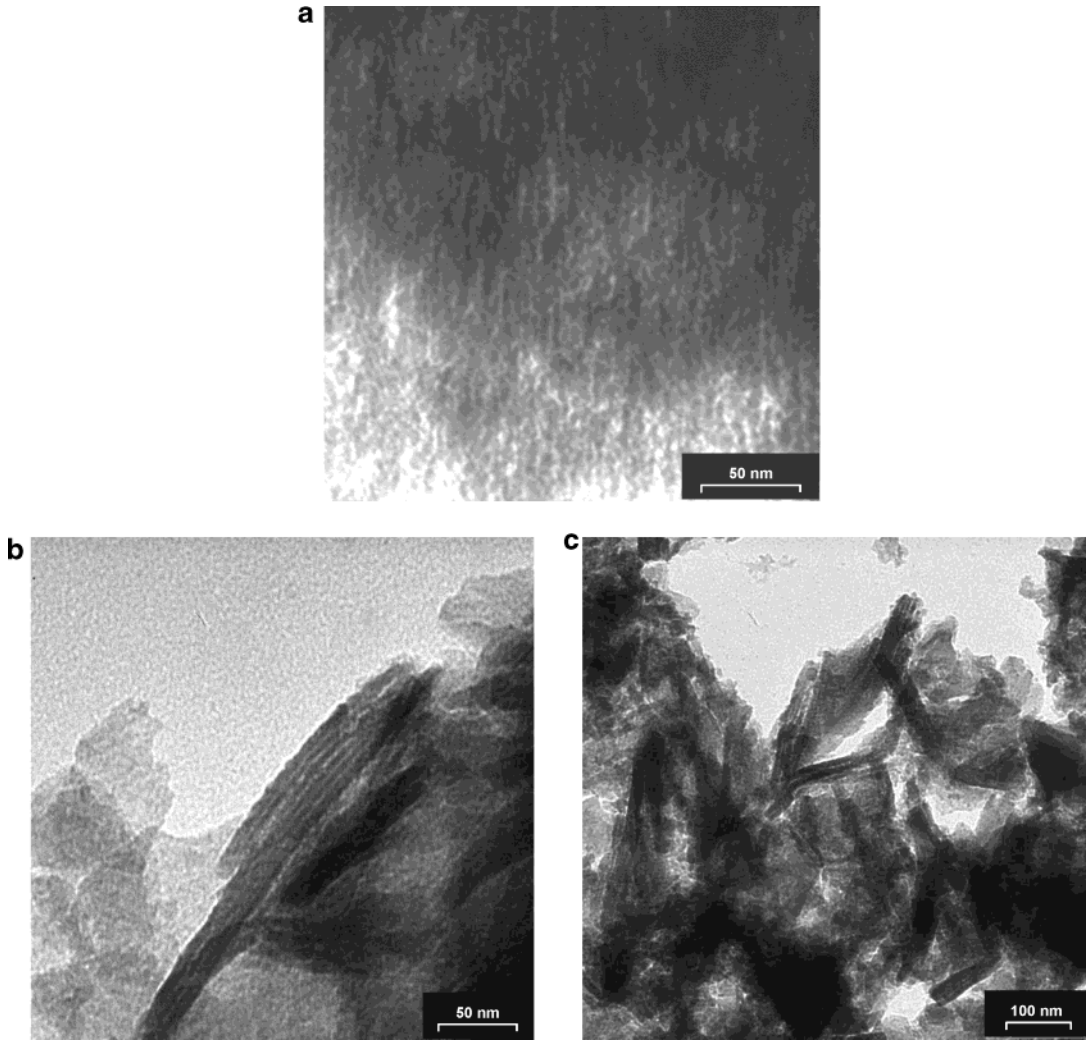

Figure 6. TEM micrographs of polyimide layers synthesized in the slitlike lamellar pores of a porous silica made by replication of the cholesteric phases of hydroxypropylcellulose as template: (a) original silica; (b, c) different micrographs of the resulting sheet like polyimide.

ment with the preceding template structure. Since only aggregates of sheets were observed, we could not decide whether the layers are covalently interconnected by rare topological defects or not. The yellow material obtained after etching with HF showed quite the same macroscopic shape as the original monolithic template, making a conclusion on the microscopic connectivity situation difficult.

WAXS measurements indicated only a slightly higher crystallinity than in the nanosphere situation, and TGA gave an even increased thermal stability of the two-dimensional system.

Conclusion

Nanoparticles and nanosheets of an aromatic polyimide were synthesized via a very simple monomer adsorption/polycondensation reaction inside the pore systems of some different mesoporous silica monoliths. The resulting nanoparticles were found as about perfect replications for both silicas under consideration: one a mesoporous silica with spherical pores with a diameter of 13 nm and another with a lamellar pore morphology with an approximately 2 nm thickness.

All analytical data as well as the thermogravimetric behavior indicated that indeed a quite pure polyimide was produced, with a somewhat lowered crystal size due to the nanoconfinement of the synthesis.

On the basis of AFM observations, the question was raised if at least some of the polyimide spheres were hollow due to incomplete loading with monomer. This question could not finally be answered in the present context.

As the nanosheet structures seemed to be cohesive and quite extended, it is promising to extend the present work to the replication of three-dimensional nanostructures, e.g., membranes or separation gels by nanocoating,[15] for the controlled design of high-performance membranes and filters with structural features on the nanoscale.

References and Notes

(1) Beck, J. S.; Vartuli, J. C.; Roth, W. J.; Leonowicz, M. E.; Kresge, C. T.; Schmitt, K. D.; Chu, C. T. W.; Olson, D. H.; Sheppard, E. W.; McCullen, S. B.; Higgins, J. B.; Schlenker, J. L. *J. Am. Chem. Soc.* **1992**, *114*, 10834−10843.

(2) Johnson, S. A.; Brigham, E. S.; Ollivier, P. J.; Mallouk, T. E. *Chem. Mater.* **1997**, *9*, 2448−2458.

(3) Frisch, H. L.; West, J. M.; Goltner, C. G.; Attard, G. S. *J. Polym. Sci., Part A: Polym. Chem.* **1996**, *34*, 1823−1826.

(4) Göltner, C. G.; Weissenberger, M. C. *Acta Polym.* **1998**, *49*, 704−709.

(5) Jun, S.; Joo, S. H.; Ryoo, R.; Kruk, M.; Jaroniec, M.; Liu, Z.; Ohsuna, T.; Terasaki, O. *J. Am. Chem. Soc.* **2000**, *122*, 10712−10713.

(6) Ryoo, R.; Joo, S. H.; Kruk, M.; Jaroniec, M. *Adv. Mater.* **2001**, *13*, 677−681.
(7) Wu, C. G.; Bein, T. *Science* **1994**, *264*, 1757−1759.
(8) Nguyen, T. Q.; Wu, J. J.; Doan, V.; Schwartz, B. J.; Tolbert, S. H. *Science* **2000**, *288*, 652−656.
(9) Wu, J. J.; Gross, A. F.; Tolbert, S. H. *J. Phys. Chem. B* **1999**, *103*, 2374−2384.
(10) Sroog, C. E. *Prog. Polym. Sci.* **1991**, *16*, 561−694.
(11) Thomas, A.; Antonietti, M. *Adv. Funct. Mater.* **2003**, *13*, 763−766.
(12) Thomas, A.; Schlaad, H.; Smarsly, B.; Antonietti, M. *Langmuir* **2003**, *19*, 4455−4459.
(13) Polarz, S.; Antonietti, M. *Chem. Commun.* **2002**, 2593−2604.
(14) Göltner, C. G.; Smarsly, B.; Berton, B.; Antonietti, M. *Chem. Mater.* **2001**, *13*, 1617−1624.
(15) Caruso, R. A.; Antonietti, M. *Chem. Mater.* **2001**, *13*, 3272−3282.

MA035804O